Available online at www.sciencedirect.com
ScienceDirect
Quaternary International 167–168 (2007) 19–34

A gradual drowning of the southwestern Black Sea shelf: Evidence for a progressive rather than abrupt Holocene reconnection with the eastern Mediterranean Sea through the Marmara Sea Gateway

Richard N. Hiscott[a,*], Ali E. Aksu[a], Peta J. Mudie[b], Fabienne Marret[c], Teofilo Abrajano[d], Michael A. Kaminski[e], James Evans[e], Ayşe İ. Çakiroğlu[a], Doğan Yaşar[f]

[a]*Department of Earth Sciences, Memorial University of Newfoundland, St. John's, NF, Canada A1B 3X5*
[b]*Geological Survey of Canada—Atlantic, P.O. Box 1006, Dartmouth, NS, Canada B2Y 4A2*
[c]*Department of Geography, The University of Liverpool, Roxby Building, Liverpool L69 7ZT, UK*
[d]*Department of Earth and Environmental Sciences, Rensselaer Polytechnic Institute, Troy, NY 12180, USA*
[e]*Department of Earth Sciences, University College London, Gower Street, London WCIE 6BT, UK*
[f]*Institute of Marine Sciences and Technology (IMST), Dokuz Eylül University, Haydar Aliyev Caddesi No.10, Inciraltı, Izmir, 35340, Turkey*

Available online 4 May 2007

Abstract

Core M02-45 recovered 9.5 m of a ~12 m-thick transgressive succession on the SW Black Sea shelf. The underlying transgressive unconformity, α, deepens toward the shelf edge, so that the coresite was never isolated from the open Black Sea. Fourteen radiocarbon dates indicate sedimentation from ~9.3 ka to the present, with only one hiatus at ~270 cm depth spanning ~4.5–2.5 ka. Three units are present in the core: Unit A (0–270 cm) = burrowed mud with laminated silt beds and mollusc shells of Mediterranean affinity (accumulation rate ~125 cm/ky); Unit B (270–525 cm) = silty mud with shelly interbeds containing *Truncatella subcylindrica*, *Mytilus galloprovincialis, Parvicardium exiguum, Rissoa* spp. and *Modiolula phaseolina* (rate ~85 cm/ky); Unit C (525–950 cm) = burrowed silty mud with graded beds of silt and fine sand, and shells of *T. subcylindrica, P. exiguum* and *Dreissena polymorpha* (rate ~360 cm/ky). Unit C developed below storm wave base at a time when proponents of a catastrophic flood in the Black Sea claim that the shelf was subaerially exposed. Clearly it was not. Ostracoda of Caspian affinity indicate ~5‰ salinity until ~7.5 ka. Dinocysts and foraminifera confirm a low but rising salinity after ~8.6 ka. An increase of δ^{34}S from ~5–30‰ through 8.4–7.6 ka is attributed to a first pulse of sulfate-rich Aegean water into an already high Black Sea, after which this sulfate was quantitatively precipitated as sulfide. δ^{34}S then dropped at ~8 ka to ~−20‰ as dysoxia and water-column stratification were established because of the initiation of two-way flow through the Bosphorus. Earlier water exchange with the Mediterranean was likely impeded by strong Black Sea outflow which prevented easy access of the Aegean water mass.
© 2006 Elsevier Ltd and INQUA. All rights reserved.

1. Introduction

Aksu et al. (2002a) described and mapped a blanket of Holocene deposits, locally >10 m thick, on the SW Black Sea shelf (Fig. 1c). These strata lie above a prominent transgressive unconformity which they called α. This unconformity corresponds to the basin-wide "washout" described by Khrischev and Georgiev (1991), created by transgression over what had been a subaerially exposed coastal plain. At the shelf edge, in water depths of ~110 m, there is a progradational delta lobe which Aksu et al. (2002a) ascribed to deposition during the sealevel lowstand associated with glacial isotopic stages 2–4; this is their lobe Δ_1. In this part of the Black Sea, water depths on the shelf exceed 60 m even within 5 km of the modern shoreline. Where water depths are less than ~50–60 m, the inner shelf is largely devoid of Holocene sediments, so that dipping and locally folded Neogene strata are exposed at the sea bed (Hiscott and Aksu, 2002).

In a recent summary of their work in the Black Sea – Marmara Sea – Aegean Sea region, Hiscott et al.

*Corresponding author.
E-mail address: rhiscott@mun.ca (R.N. Hiscott).

1040-6182/$ - see front matter © 2006 Elsevier Ltd and INQUA. All rights reserved.
doi:10.1016/j.quaint.2006.11.007

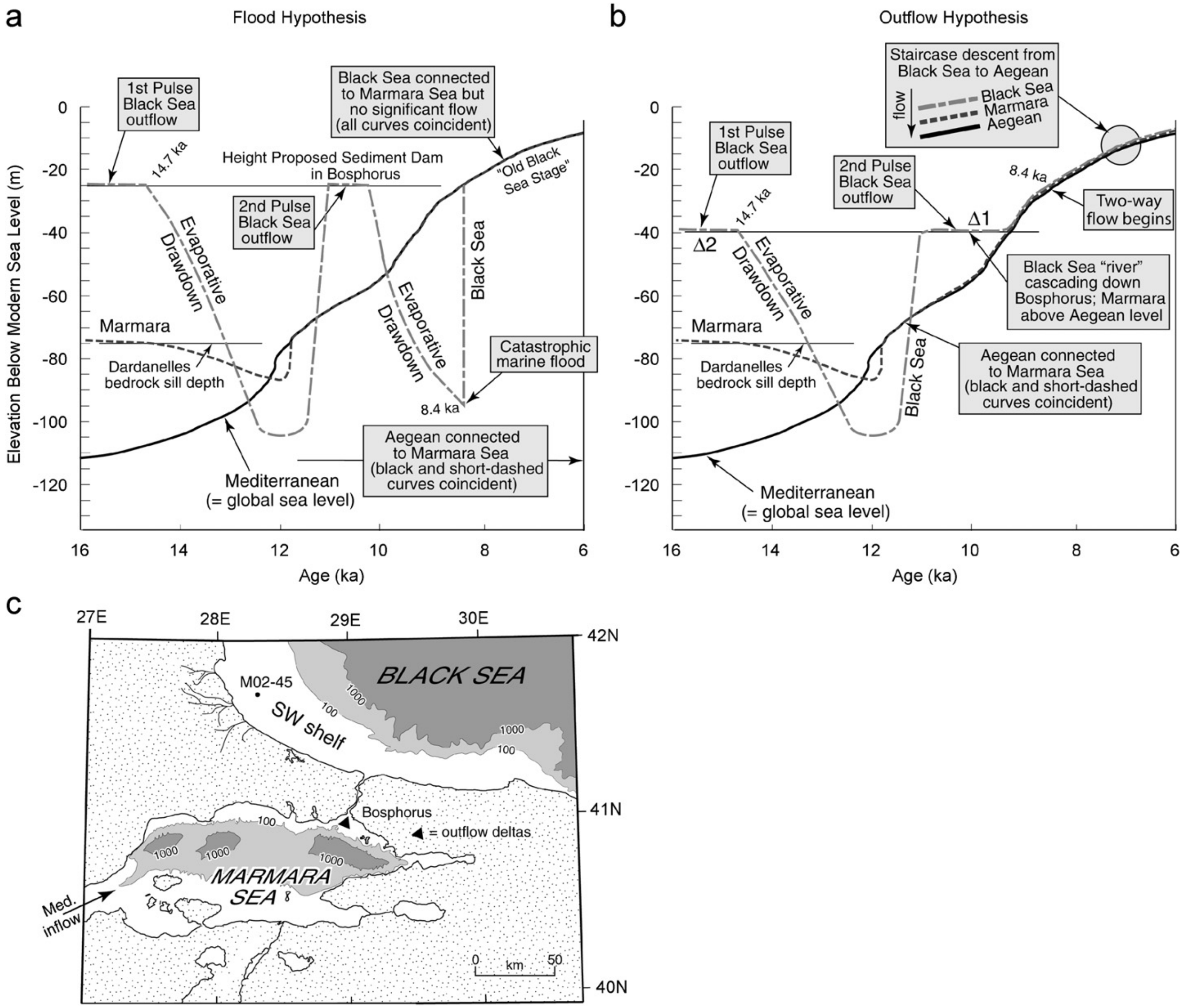

Fig. 1. Schematic water-level histories of the Black Sea, Marmara Sea, and Mediterranean (Aegean) Sea according to the *Flood Hypothesis* ((a), Ryan et al., 2003) and the *Outflow Hypothesis* ((b), Hiscott et al., 2007). Δ1 and Δ2 are Black-Sea-outflow deltas south of the Bosphorus Strait in the northern Marmara Sea ((c), Hiscott et al., 2002). In both graphs, the Mediterranean curve is the Barbados (global) curve of Fairbanks (1989). When Mediterranean and Marmara curves are superimposed (e.g., from ~12 to 10 ka in both plots), the Marmara Sea was an embayment of the Mediterranean. According to the Flood Hypothesis, Mediterranean waters catastrophically flooded into the depressed Black Sea basin when a hypothetical sediment dam in the Bosphorus channel was scoured away. According to the Outflow Hypothesis, the Black Sea reached a −40 m bedrock sill depth in the Strait of Bosphorus first, initiating a cascade downslope into the rising Marmara Sea from ~10 to 9 ka and the construction the outflow delta Δ1 at the southern exit of the strait (Hiscott et al., 2002; Aksu et al., 2002b). This hypothesis does not involve a catastrophic flood. (c) Simplified map of the SW Black Sea and links to the Mediterranean through the Bosphorus Strait. Water depths are in meters.

(2007) highlighted the stark disagreement that exists between their view that the Black Sea has been spilling into the Marmara Sea through the Bosphorus Strait since ~10–11 ka (the *Outflow Hypothesis*), and the proposal by Ryan et al. (1997, 2003) and Major et al. (2006) that the level of the Black Sea stood at ~−95 m when it was catastrophically inundated by Mediterranean waters at ~8.4 ka (the *Flood Hypothesis*—uncalibrated ^{14}C ages are used throughout this paper). The contrasting views of recent water levels and connections are summarized in Figs. 1a and b. In order for the Black Sea to have been spilling through the Bosphorus Strait by ~10–11 ka, its level must have been shallower than ~−40 m based on the present sill depth in the strait and the elevation of the top of an overspill delta south of the strait on the NE shelf of the Marmara Sea (Aksu et al., 2002b; Hiscott et al., 2002). Ryan et al. (2003) agree that this early overspill took place, and provide evidence for a somewhat shallower spill depth of ~−30 m. They advocate, however, that the level of the Black Sea then fell because of increased aridity to reach

~−95 m by 8.4 ka. One complication with this scenario of a lowstand immediately before 8.4 ka is that the level of the global ocean reached −40 m at ~9.5 ka and −30 m at ~9.0 ka (Fairbanks, 1989). It is therefore not clear what kept Mediterranean waters from entering the Black Sea earlier than 8.4 ka, particularly if the Bosphorus sill depth had been in the range of −40 to −30 m only a short time before. Ryan et al. (1997) had advocated a sediment dam in the Bosphorus to explain the delayed flooding, but we cannot imagine what process would have created this barrier in the short time interval between ~10 and ~9 ka.

As illustrated by Fig. 1, the nub of the disagreement between our group on the one hand, and Ryan et al. (2003) and Major et al. (2006) on the other, concerns the time period from ~10 to 8.4 ka. Our *Outflow Hypothesis* holds that the Black Sea remained high. Their *Flood Hypothesis* identifies a sharp drawdown throughout this interval of time to ~−95 m, producing an unconformity within the Holocene shelf deposits (unconformity 1a of Ryan et al.(2003), which they correlate with unconformity α_1 of Aksu et al.(2002a)). Several workers from eastern European countries also dispute that an early Holocene sea-level drawdown and catastrophic flood occurred (Fedorov, 1982; Chepalyga, 1984; Filipova-Marinova, 2006; Yanko-Hombach, 2006). Instead, they advocate a gradual and in some cases step-wise Holocene rise in the level of the Black Sea, reaching depths shallower than ~−40 m by ~9–9.5 ka and never dropping below that level again.

In 2002, we cored 9.5 m into the post-transgressive succession on the SW Black Sea middle shelf at a water depth of 69 m (Fig. 1c). Core M02-45 establishes conclusively that the level of the Black Sea was shallower than ~−70 m by ~9.3 ka and remained so until the present. Sedimentary facies, decribed below, suggest that the water depth was actually shallower than ~−55 m. The thickness of unpenetrated strata below the base of the core suggests that the transgression began no later than ~10 ka. There are two unconformities within the Holocene succession, but new radiocarbon dates reported below indicate that they formed at ~7.5 ka (α_1) and in the time interval ~2.5–4.5 ka (α_2), well after both the proposed water-level drawdown of Ryan et al. (2003) and Major et al. (2006) and their estimated time of catastrophic flooding. These are therefore not transgressive unconformities produced by shoreface erosion (i.e., ravinement surfaces). Instead, we attribute α_1 and α_2 to marine erosion during phases of local intensification of the Rim Current (Oğuz et al., 1993). This interpretation disagrees with our earlier views (Aksu et al., 2002a, pp. 74 and 79), in which we proposed that α_1 was a lowstand unconformity and α_2 was a ravinement surface.

In this manuscript, we present proxy data from core M02-45 which demonstrate brackish conditions on an open SW Black Sea shelf from ~9.5–7.5 ka. A minor pulse of Mediterranean water (or short series of pulses) reached the Black Sea almost 1000 years earlier at ~8.4 ka (Major, 2002; Mudie et al., 2002a, 2004; Ryan et al., 2003; Major et al., 2006), but was short-lived based on our core results. Sustained two-way flow began at ~7.5 ka when faunal assemblages and dinocysts indicate a rise in salinity to >10–12‰. Strong stratification and anoxia/dysoxia were established by ~2.4 ka. These results substantiate our earlier views that (a) the level of the Black Sea rose to its spillover point by ~10 ka, (b) this level has not dropped significantly since, and (c) the re-establishment of a Holocene connection between the Mediterranean Sea and Black Sea was gradual and progressive, not catastrophic.

2. Seismic stratigraphy of the post-transgressive succession, SW Black Sea shelf

We have remapped three Holocene seismic units in the vicinity of coresite M02-45, using a grid of ultra-high resolution Huntec deep-tow-system (DTS) boomer profiles acquired with an average line spacing of ~2 km on the inner and middle shelf and ~4 km on the outer shelf. The Huntec DTS profiles were collected using a deep-tow system with a 500 J boomer source, recorded using both a single internal hydrophone and a 21-element 6 m-long Benthos hydrophone streamer. The Huntec DTS profiles have a vertical resolution of 15–30 cm, and locally provide details on sedimentary deposits up to 50–100 m below the seabed. The remapped seismic units correspond to seismic units 1B, 1C and 1D of Aksu et al. (2002a); their seismic unit 1A is only present at the shelf edge and consists of lowstand delta lobes. On the middle shelf, 1B directly overlies the transgressive unconformity, α. 1C overlies a widespread reflection called α_1 that is locally an erosional unconformity. 1D overlies a second unconformity, α_2, that is in most profiles an onlap surface. At coresite M02-45, seismic data provide no evidence for an hiatus at α_1, whereas α_2 is an onlap surface.

Seismic unit 1B consists of discontinuous, subtly mounded, moderately strong reflections just above α, passing quickly upward into weaker but very continuous reflections that characterize the bulk of the unit (Fig. 2). This reflection configuration is characteristic of stratified muds, although the basal hummocky and more reflective deposits are likely more sand-prone. A structure-contour map of the α unconformity surface shows that deposition occurred in a semi-enclosed shelf depression which opened toward the north (Fig. 3), affording unrestricted communication between the middle shelf and the open Black Sea basin. An isopach map of unit 1B (Fig. 4a) shows it to be thickest on the middle shelf and thin to absent over the shelf-edge high that partially enclosed the middle shelf depression. Aksu et al. (2002a) defined unit 1B closer to the shelf edge where it is thinner and likely has a younger basal age.

Seismic unit 1C has a distinctive acoustic character, consisting of moderately strong but highly discontinuous and "crinkly" reflections. On other parts of the shelf, it passes laterally into morphological mounds interpreted as mud volcanoes by Aksu et al. (2002a; their Fig. 17). In the

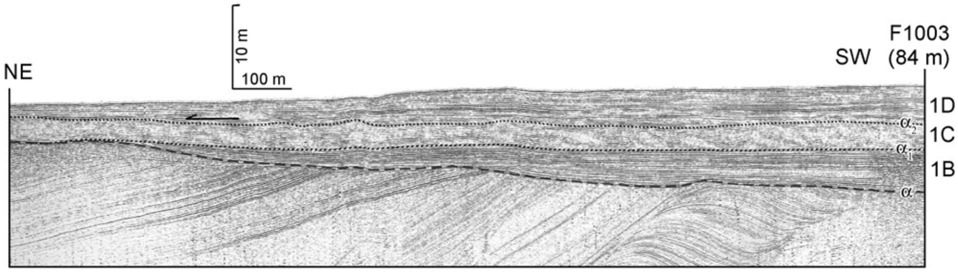

Fig. 2. Huntec DTS boomer profile showing the acoustic properties and geometries of seismic units 1B–1D. The profile is located in Fig. 3. Seismic unit 1B onlaps α toward the NE in this area because there is a shelf-edge paleo-bathymetric high. At the SW extremity of the profile, continuous high- to moderate-amplitude reflections in unit 1B are obscured by gas. Seismic unit 1C has a characteristic hummocky/crinkly character, wherease unit 1D is similar to unit 1B, but with less consistently parallel reflections. Elsewhere, seismic unit 1D is characterized by large climbing waveforms and drift-like deposition around mud volcanoes. Note that unit 1D subtly onlaps unit 1C toward the NE.

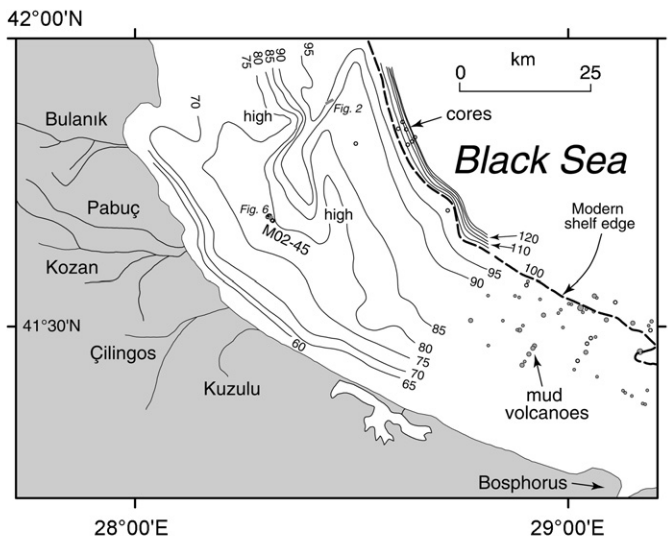

Fig. 3. Structure-contour map at the level of unconformity α. Contoured values are in meters below sealevel. Two paleo-highs partly protected coresite M02-45 from the open sea at ~9 ka, but these highs would have been entirely submerged if water depth at the coresite was even 10 m. Rivers draining from the west and southwest of coresite M02-45 supplied shelf-edge deltas during lowstands. The locations of short seismic profiles shown in Figs. 2 and 6 are indicated.

vicinity of coresite M02-45, this unit has a sheet-like geometry with only gradual thickness changes (Fig. 4b). The top of seismic unit 1C is marked by onlap in almost all seismic profiles.

In the vicinity of coresite M02-45, seismic unit 1D is very similar in reflection character and continuity to unit 1B. Elsewhere on the shelf, particularly to the southeast and near the shelf edge, it forms drift-like deposits around elevated mud volcanoes and shelf ridges, and contains many internal truncation surfaces (Aksu et al., 2002a, their Fig. 19). The thickest deposits of unit 1D (Fig. 4c) are offset from the thickest deposits of seismic unit 1B (Fig. 4a; see also Hiscott and Aksu, 2002, their Fig. 16, with their * reflection equivalent to α_1—on their Fig. 2d location map, Hiscott and Aksu (2002) mislabelled this profile as "Fig. 15").

3. Chronology of core M02-45

A short trigger-weight core (i.e., gravity core; M02-45TWC) and piston core (M02-45P) were collected at 41°41.17′N, 28°19.08′E. Radiocarbon dates in both cores (Table 1) indicate some core-top loss in the piston core. This is a normal outcome during piston coring, because water-rich surface sediments are easily bypassed by the heavier corer, and because of uncertainties in setting the trip-wire length when rigging the corer. Our best matches of radiocarbon ages and geochemical trends suggest that a depth of 110 cm in the trigger-weight core is equivalent to the top of the piston core. All depths in this paper are given relative to the seafloor at the coresite, with the result that the top of the piston core has been adjusted downward to a depth of 110 cm to account for the core-top loss. The composite succession obtained by splicing together records from the trigger-weight and piston cores is designated as core M02-45.

A plot of radiocarbon dates against depth (Fig. 5) indicates accumulation rates of ~360 cm/1000 yr from 605 to 950 cm depth, ~85 cm/1000 yr from 330 to 605 cm depth, and ~125 cm/1000 yr in the upper 268 cm of the composite core. The age discontinuity between 268 and 330 cm correlates with the approximate depth of α_2 (Fig. 6)—based on facies in the core, α_2 is correlated to a core depth of 270 cm. The youngest deposits beneath α_2 have an age of ~4.5 ka and the duration of the hiatus is ~2000 years (Fig. 5). There is no apparent hiatus at α_1, but correlation of the dated core to the seismic data suggests an age of ~7500 yr BP. Farther east on the southern Black Sea shelf, Mart et al. (2006) identify an equivalent unconformity which is overlain by sediments younger than 4400 yr BP.

Unconformity α is believed to be at least 250 cm below the base of core M02-45 (Fig. 6). Based on accumulation rates, α is therefore inferred to be at least 700 years older than the deepest recovered sediments. This provides a

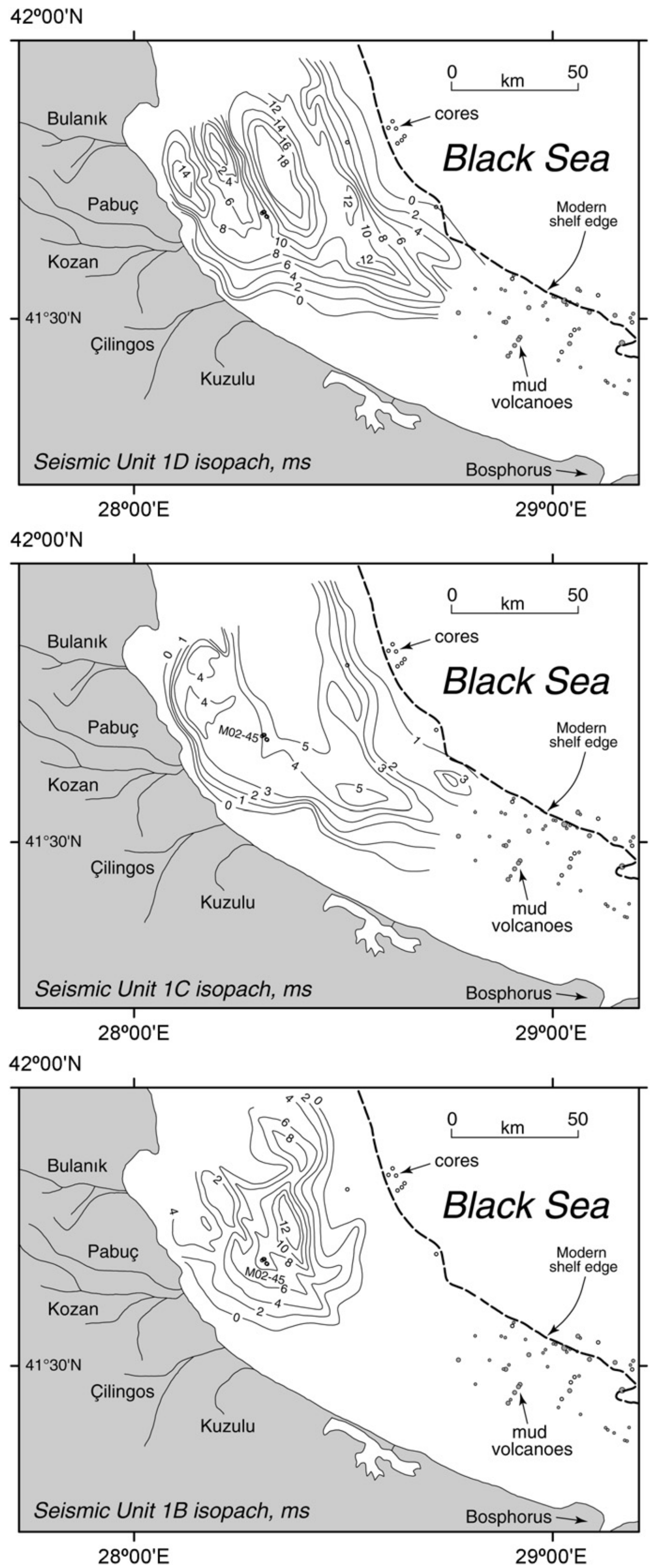

Fig. 4. Isopach maps of seismic units 1B (lower), 1C (middle) and 1D (top). The contoured values are in milliseconds (TWT), with 10 ms ~7.5 m of sediment. Coresite M02-45 is labelled in the lower and middle panels. This and other cores are indicated by unfilled circles. Mud volcanoes are indicated by gray-filled circles.

minimum age of ~10 ka for α. The approximate ages of seismic units 1B, 1C and 1D are therefore 10–7.5 ka, 7.5–4.5 ka, and 2.5–0 ka, respectively.

4. Methods of core analysis

Core M02-45 was split and described after upright shipment from Turkey to Canada. Texture, color and sedimentary structures were evaluated visually. 20 cm^3 samples were taken each 10 cm for micropaleontological, textural, and geochemical analysis. Samples were wet sieved through a 63 μm screen to determine the proportion of sand and to isolate foraminifera, ostracods and mollusc shells for subsequent identification. For benthic foraminiferal studies, the dry sand fraction was screened once more at 125 μm, then split with a microsplitter until a subsample containing about 300–400 specimens was obtained. This step was omitted if the entire sample was judged to contain fewer than 300 specimens. For particularly rich samples, microsplitting reduced the >125 μm fraction to one-eighth to one-sixteenth of its original size. We did not use any heavy liquids to concentrate the foraminifera. Instead, 100% of the visible foraminifera were hand picked from the split of the >125 μm fraction according to standard procedures. The number of specimens per sample averaged 290 above a core depth of 500 cm; deeper samples were impoverished and no benthic foraminifera were seen below a depth of 620 cm. Benthic foraminifera were identified using the taxonomy of Yanko and Troitskaya (1987). All specimens in each hand-picked mount were identified and counted.

The 63–125 μm fraction of each sample was checked for the occurrence of small foraminifera, but not picked. Scant numbers of small foraminifera were seen in this fraction, not enough to affect the percentage data reported in this paper.

Sample preparation for palynology and carbon geochemistry followed procedures in Mudie et al. (2002a), and Abrajano et al. (2002). For some types of quantitative work (e.g., palynological counting), alternate samples rather than all samples were studied in intervals of lesser interest (e.g., uppermost Holocene).

The amount of total sulfur (TS) and the sulfur isotopic composition were determined using a Carlo-Erba NA 1500 Elemental Analyzer coupled to a Finnegan MAT 252 isotope-ratio mass spectrometer (IRMS). Samples were acidified using 30% HCl, and carbonate-free residues were dried overnight in an oven at 40 °C. A small amount of sample (~15 mg) was transferred into 4 × 6 mm tin capsules which were then sealed in preparation for analysis. Total sulfur in the samples was converted to SO_2, H_2O and other oxidized gases in the oxidation chamber and then passed through a reduction reagent, a $Mg(ClO_4)_2$ water trap and a 1.2 m Poropak QS 50/80 chromatographic column at 70 °C for final isolation. Total sulfur quantification from measurement of generated SO_2 was accomplished using an external standard (sulphanilamide, $C_6H_8N_2O_2S$) and a

Table 1
Radiocarbon ages for core M02-45 reported as uncalibrated conventional ^{14}C dates in yr BP (half-life of 5568 years; errors represents 68.3% confidence limits)

Core	Depth (cm)	Composite depth (cm)	Material dated	Age (yr BP)	Lab number
M02-45TWC	92	92	*Spisula subtruncata*	730 ± 50	TO-11433
M02-45TWC	145	145	*Spisula subtruncata*	770 ± 50	TO-11434
M02-45P	33	143	*Spisula subtruncata*	730 ± 40	TO-11435
M02-45P	158	268	*Mytilus galloprovincialis*	2400 ± 60	TO-11006
M02-45P	220	330	*Mytilus galloprovincialis*	5190 ± 50	TO-11436
M02-45P	302	412	*Mytilus galloprovincialis*	5900 ± 60	TO-11437
M02-45P	406	516	*Anadara* spp.	7560 ± 60	TO-11438
M02-45P	495	605	*Truncatella subcylindrica*	8380 ± 70	TO-11142
M02-45P	569	679	*Anadara* spp.	8570 ± 70	TO-11439
M02-45P	639	749	*Anadara* spp.	8620 ± 70	TO-11440
M02-45P	754	864	*Dreissena polymorpha*	8840 ± 70	TO-11441
M02-45P	810	920	Bivalve	9370 ± 70	TO-11007
M02-45P	822	932	*Dreissena polymorpha*	9340 ± 70	TO-11442
M02-45P	835	945	*Cyclope donovani*	9070 ± 70	TO-11443

TO = IsoTrace Radiocarbon Laboratory, Accelerator Mass Spectrometry Facility, University of Toronto. TWC = trigger-weight core; P = piston core.

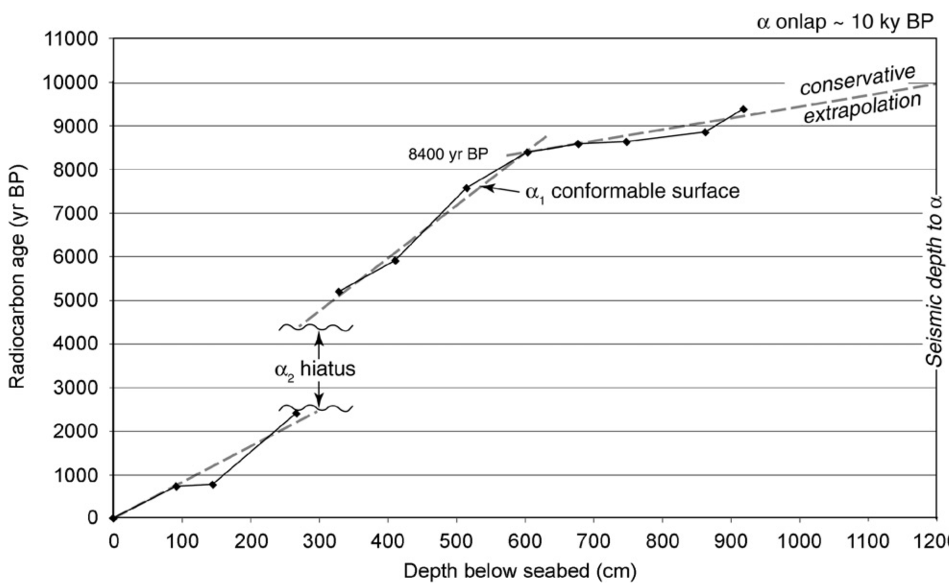

Fig. 5. Plot of radiocarbon ages against depth in the composite core M02-45. Dashed gray lines are hand-fitted trends used to calculate average sedimentation rates. The hiatus at ~270 cm core depth is inferred from (i) the offset in the sedimentation-rate trends, and (ii) the presence of onlap at this depth below the seafloor (Fig. 6). See text for discussion.

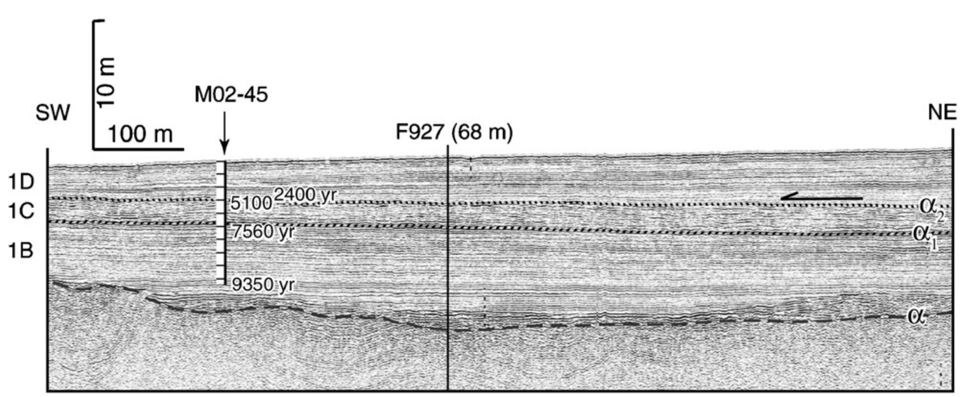

Fig. 6. Huntec DTS boomer profile over coresite M02-45, with the cored interval marked, subdivided into meters, and annotated with selected radiocarbon dates from Table 1. α is an erosional unconformity, α_1 is a conformable surface at this site but an unconformity elsewhere, and α_2 is a disconformity buried by the onlapping deposits of seismic unit 1D. The one-sided arrow indicates onlap. The profile is located in Fig. 3.

thermal conductivity detector (TCD). From the TCD, the SO_2 was carried by He to a ConFloII interface, which allows a portion of the He and combustion gases to enter directly into the ion source of the IRMS for sulfur isotopic measurement. The total sulfur concentration in the samples is back-calculated as a percentage of dry-weight sediment. All isotopic analyses are reported in standard notation referenced to the standard CDT.

Ostracods were hand picked from a split of the $>63\,\mu m$ fraction and identified using reference texts such as Athersuch et al. (1989) and Schornikov (1967). In most samples, several hundred to >1000 specimens were identified and counted. Mollusc shells were identified using a number of taxonomic keys, descriptions and illustrations (Tebble, 1966; Graham, 1971; Poppe and Goto, 1991; Grossu, 1995; Müller, 1995; Abbott and Dance, 1998; Demir, 2003), with details provided in Çakiroğlu (2005).

5. Core data

5.1. Sedimentary facies and molluscan assemblages of core M02-45

Three lithologic units are recognized in core M02-45 (Fig. 7). The oldest Unit C extends from the base of the cored interval to a depth of 525 cm. Its top therefore correlates in the seismic data to α_1 (Fig. 6). Unit B extends upward from this point to a core depth of 270 cm, which is just below a <5 cm-thick shelly horizon, and which correlates in the seismic data to α_2. Unit A coincides with seismic unit 1D. Lithologic units are described in stratigraphic order, from oldest to youngest.

Unit C consists of color-banded mud with graded laminae and beds of silt to very fine sand (Fig. 8a), and scattered shells of *Truncatella subcylindrica, Parvicardium*

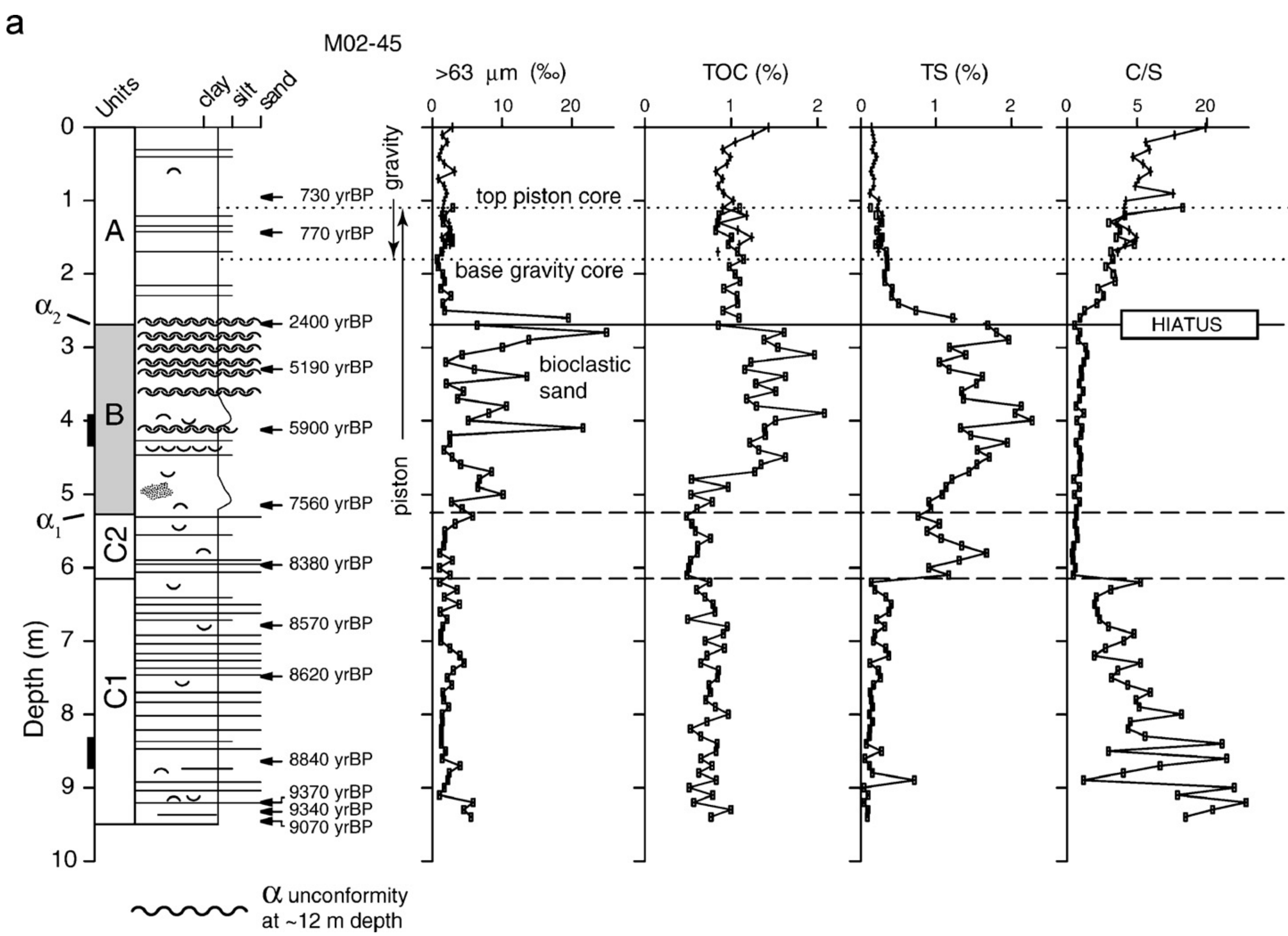

Fig. 7. Textural and geochemical proxies plotted against the sedimentary profile for core M02-45. No trends are extended across the α_2 hiatus. Inverted and upright dish-shaped symbols in the lithological column indicate shells. Units, subunits and correlations to key reflections are indicated. (a) texture and elemental abundances of organic carbon (TOC) and total sulfur (TS). Bold lines adjacent to the depth scale in part (a) indicate the position of core photographs shown in Fig. 8. (b) carbon and sulfur isotopic compositions. Terrigenous fraction of the TOC is estimated by assuming that the bulk $\delta^{13}C$ constitutes a mixture of marine and terrigenous end-members with $\delta^{13}C$ ratios of −22‰ and −27‰, respectively (Aksu et al., 1999b). See text for discussion.

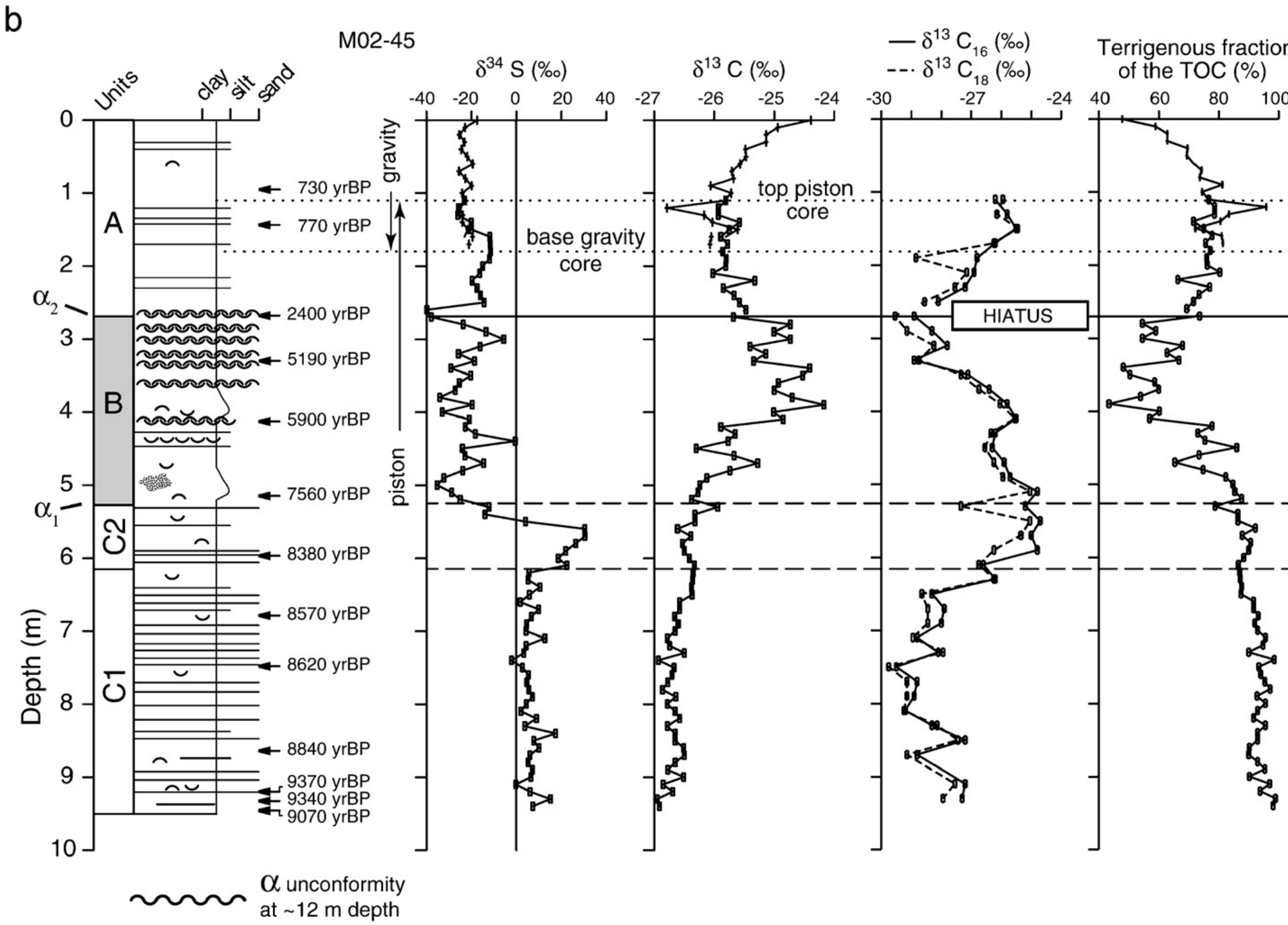

Fig. 7. (*Continued*)

exiguum and *Dreissena polymorpha*. It is divided into Subunit C1 below 615 cm and Subunit C2 from 525 to 615 cm, based on geochemistry rather than facies (see below). The shallowest occurrence of *D. polymorpha* is at a core depth of 600 cm (age = ~8400 yr BP); below 615 cm, it accounts for 33% of all recovered shells. *Truncatella subcylindrica* and *Parvicardium exiguum* live today in the Mediterranean and Black Seas, and have wide salinity tolerance. *D. polymorpha* is endemic to the Pontic-Caspian region and indicates brackish waters (salinity < 15‰).

Unit B consists of alternating horizons of mud and shelly mud (Fig. 8b). The abundance of bioclastic sand locally exceeds 20% (Fig. 7a). The mollusc assemblage includes *T. subcylindrica*, *Mytilus galloprovincialis, P. exiguum, Rissoa* spp. and *Modiolula phaseolina*. The first three species are the most common, accounting for 83% of all recovered shells. *M. galloprovincialis* dominates the shelly layers in the upper part of the unit; its lowest occurrence is at a core depth of 470 cm. *M. phaseolina* suggests salinities of ~18‰ during Unit B time.

The youngest Unit A consists of color-mottled/banded, burrowed mud with silt laminae and scattered shells of several immigrant Mediterranean molluscs: *Bittium reticulatum, Spisula subtruncata, Acanthocardia paucicostata, Abra alba, M. galloprovincialis, T. subcylindrica*, and *Turritella communis*. The low-salinity indicator *Dreissena polymorpha* was found in only one sample.

The sharp-based, graded thin sand and silt interbeds in Unit C are event deposits, either storm deposits (tempesites) or turbidites. In a shelf setting, turbidites are only prevalent in prodelta deposits. Aksu et al. (2002a) have mapped a number of lowstand shelf-edge deltas in the study area, and point to a set of modern rivers as the source of fluvial input during lowstands. Today, these rivers have separate mouths (Fig. 3), but at lowstands might have coalesced, while crossing the shelf, into a single drainage network. Even after the onset of the Holocene transgression, river mouths would have periodically sourced delta-front turbidity currents either during flood stages, or as a result of the failure of oversteeped mouth bars. The graded beds of Unit C lack any evidence of wave reworking or rippling. This suggests that deposition occurred below storm wave base. Today, storm wave base is ~−95 m (Aksu et al., 2002a). During Unit C time, however, the

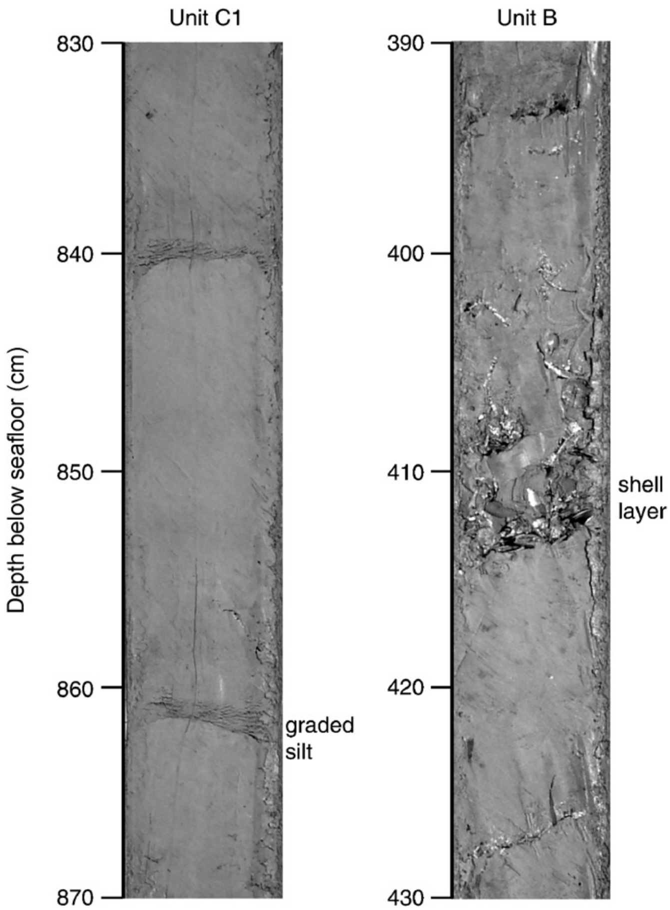

Fig. 8. Photographs of typical features of lithologic units C1 (left) and B (right). The graded silts and very fine sands in Subunit C1 punctuate burrowed muds; these graded beds are interpreted as prodelta turbidites which accumulated below storm wave base. The shell layers in Unit B are dominated by *Mytilus galloprovincialis*. The locations of these photographs are marked in Fig. 7a.

middle shelf was somewhat protected from offshore swell by the paleo-bathymetric high seaward of coresite M02-45 (Fig. 3), but it is still likely that storm wave base was deeper than ~30 m. With a modern water depth of 69 m and Unit C sub-seafloor depths of ~9 m, the 9 ka water depth in the vicinity of coresite M02-45 is interpreted to have been shallower than $69+9-30=48$ m. Based on the paleo-bathymetry (Fig. 3), the 9 ka shoreline in the SW Black Sea would have been within 5 km of the modern coastline.

Unit B muds and shelly muds with a diverse molluscan fauna suggest well oxygenated marine conditions. We have encountered such interbedded muds and shelly muds in many cores on the Black Sea shelf, over a wide geographic area (Aksu et al., 2002a, their Fig. 23). The shells show no evidence of significant transport or abrasion, so we interpret them as thin, *in situ* mollusc communities living on a mud bottom. The decreased abundance of macro-fauna and the sharp decline in TS in Unit A suggest reduced oxygen levels in the basin as a whole after ~2.4 ka, with sulfur drawdown attributed to precipitation of pyrite in deeper parts of the now-anoxic Black Sea basin.

5.2. Carbon and sulfur geochemistry

In Subunit C1, total organic carbon (TOC) is rather uniform at 0.5–1.0% (Fig. 7a); this is ~90% terrigenous carbon and ~10% marine carbon (Fig. 7b). δ^{13}C of the TOC is mostly −26.5‰ to −27‰, and compound-specific carbon isotopic signatures (C16 and C18 saturated fatty acids) are even more negative at ~−28‰ to −29‰ (Fig. 7b). TS is less than 0.5% and δ^{34}S is uniform in the range 0–10‰. In Subunit C2, TOC is ~0.5% and remains ~85–90% terrigenous in origin. δ^{13}C of the TOC is ~−26.5‰, whereas C16 and C18 saturated fatty acid δ^{13}C values climb to higher values than in Subunit C1, eventually reaching ~−26‰ to −25‰. Such profound shift in fatty acid δ^{13}C values is commonly ascribed to limitation in the supply of carbon substrates during primary production. Unlike total organic carbon, the sulfur composition is dramatically different to values in Subunit C1. TS rises rapidly at the base of Subunit C2 to values >1%, reaching a peak of ~1.7% by the middle of the subunit (~8200 yr BP) before declining to ~1% at the top. The increased TS is marked by abundant fine pyrite particles, less than 5 μm in diameter, in palynological separates (Mudie et al., this volume). δ^{34}S increases progressively throughout the lower part of Subunit C2, reaching values of ~30‰ (marginally higher than seawater sulfate; Paytan et al., 1998). There is then a steady decline in δ^{34}S across the interval 560–525 cm to values of ~−20‰. The change is large—about 50‰! Based on accumulation rates, this large decline in δ^{34}S occurred over a time interval of ~500 years.

TOC is ~0.5% at the base of Unit B but more than doubles to ~1.5% above a core depth of 480 cm (Fig. 7a). The marine contribution to the TOC increases to ~50% in the middle to upper part of Unit B—such values are distinctly different to the source compositions for Units C and A, and are only seen again at the modern depositional surface (Fig. 7b). There is a rise in values of δ^{13}C from −26.2‰ to ~−25‰ which parallels the rise in TOC. δ^{13}C has peaks as high as −24.2‰ (Fig. 7b). In contrast, the compound-specific δ^{13}C values for C16 and C18 fatty acids gradually *decrease* through Unit B from ~−25‰ to ~−29‰. TS increases progressively from ~1% to ~2% in the lower half of the unit, and then fluctuates irregularly in the range 1–2%. δ^{34}S fluctuates from ~−40‰ to ~0‰, with an average of ~−20‰. Poorly defined trends might exist in the δ^{34}S profile through Unit B, but these are masked by the scatter in the data.

TOC is uniform at ~1.0% in Unit A (Fig. 7a). The proportion of terrigenous organic matter is ~75% except for the upper 100 cm of the composite core. Above this depth, the proportion of marine organic carbon increases gradually to ~50%, in step with a gradual increase in δ^{13}C to ~−24.5‰. Below this depth, δ^{13}C shows weak trends in the range −25.5‰ to −26‰. δ^{13}C values for C16 and C18 fatty acids are higher in the base of Unit A than they are in the top of Unit B, but this offset is to be expected since there is an hiatus of ~2000 years at the contact between these units. Samples from the trigger-weight core were not analyzed, but we expect an upward continuation of the same inverse relationship seen in Units B and A between bulk δ^{13}C and compound-specific (C16 and C18 fatty acid) values of δ^{13}C. δ^{34}S is essentially unchanged from the values of about −20‰ seen in Unit B, except for an excursion to −40‰ at the α_2 hiatus. TS decreases upward through Unit A from ~1.2% to ~0.2%.

5.3. Microfossils and their constraints on water-mass characteristics

There are no planktonic foraminifera in our samples, consistent with the low salinity of Black Sea surface waters and the strong surface-water outflow through the Bosphorus Strait. We did not study coccoliths and diatoms. Foraminifera are very rare in Unit C, consisting of individual specimens of *Ammonia* and *Porosononion*. These might have been mixed downward into Unit C by burrowers. The high abundance of pyritized burrow infillings in Unit C appears to support this interpretation. Organic linings of benthic foraminifera, however, are common in palynological residiues at intervals in Unit C, suggesting that dissolution might also have contributed to the low number of foraminifera. Likewise, organic linings of ostracoda in palynological residues point to local carbonate dissolution.

Ammonia species display high dominance in Unit B (Fig. 9a), where *Ammonia tepida* is the most abundant species. The diversity of this assemblage is lower than in Unit A (with a maximum of 7 species, versus 17 species in Unit A). Accessory species are rare, and mostly consist of *Porosonion* sp. The shallowest consistent occurrence of lagenids is noted at a composite core depth of 390 cm (~5800 yr BP from Fig. 5), indicating deposition in a shelf environment with water depths in excess of ~35 m (see Yanko and Troitskaya, 1987, their Table 6). An assemblage dominated by *A. tepida* (without lagenids) today characterizes areas of the inner continental shelf off Bulgaria where salinity values are in the range of 17–19‰ (Yanko, 1990).

Benthic foraminifera and ostracods with Mediterranean affinities are relatively diverse in Unit A. The foraminiferal assemblage in this unit is dominated by *A. compacta*, with lesser numbers of *A. tepida* (Fig. 9a). These are accompanied by *Haynesina depressula* and *H. germanica*, *Gavelinopsis praegeri*, *Elphidium* spp., lagenids, and sporadic occurrences of agglutinated taxa (mostly *Eggerelloides scabrus*, *Ammomarginulina* sp., and *Reophax* sp.). Miliolids are rare and mostly consist of the genus *Triloculina*. The miliolids and agglutinates are confined to Unit A. Yanko (1990, Table 1) indicates that *A. compacta* is a relatively deep-water form which characterizes areas deeper than ~70 m on the modern Bulgarian outer shelf; there, the salinity is 21–22‰.

Ostracods are found from the core top downward, well into Unit C, but the ostracod species change from an exclusively Mediterranean assemblage above 420 cm (in Unit B) to a Caspian (brackish) assemblage below 500 cm (implied salinity ~5‰; Evans, 2004); the intervening 80 cm interval contains a mixture of these two assemblages and therefore has the highest ostracod diversity in core M02-45 (Fig. 9b). The time required to complete this transition in ostracod assemblages was ~1300 years, from ~7300 to 6000 yr BP (Fig. 5).

Dinoflagellate cysts and colonial algae (*Pediastrum, Botrycoccus*) provide the clearest record of changing water-mass characteristics (Fig. 9; Mudie et al., this volume). The freshwater algae *Pediastrum* and *Botrycoccus* are only significant below a depth of 510 cm (age ~7500 yr BP). In the same interval and upward to a depth of 460 cm (age ~6700 yr BP), a dinocyst assemblage dominated by *Spiniferites cruciformis* and *Pyxidinopsis psilata* indicates brackish waters with salinities of 3–12‰. Flickering, minor amounts of euryhaline/Mediterranean species in the same interval indicate periodically increased salinity. We interpret the overlap of *Pediastrum* and the *S. cruciformis* assemblage to indicate brackish conditions throughout Unit C time, with the freshwater species washed in from rivers or nearby coastal areas.

Mediterranean dinocysts *S. belerius, S. bentorii, S. mirabilis, S. ramosus* and *Operculodinium centrocarpum* first appear in a persistent way at a depth of 510 cm (~7500 yr BP), reaching their highest relative proportions

Fig. 9. Microfossils and ostracods plotted against the sedimentary profile for core M02-45. No trends are extended across the α_2 hiatus. (a), Benthic foraminifera abundances. Only unidentifiable foramiferal linings are present in Unit C below 670 cm (~8500 yr BP); hence, the deeper part of the core stratigraphy is not presented in this part of the figure. Species abundances are presented as a percentage of all benthic foraminifera in each sample. Polyhaline species (Yanko, 1990) are found in environments where the salinity is in excess of 11‰, and include *Gavelinopsis praegeri*, *Fissurina ex gr. lucida*, and *Eggerelloides scabrus. A. tepida* is an inner shelf dweller in salinities of 17–19‰, whereas *A. compacta* lives in deeper water (>70 m) with salinities of 21–22‰ (Yanko, 1990). (b), Freshwater algae = *Pediastrum simplex* + *P. boryanum* + *Pediastrum* sp. + *Botryococcus*; *S. cruciformis* group = *Spiniferites cruciformis* + *Pyxidinopsis psilata* + *S. inaequalis*; *Lingulodinium machaerophorum sensu lato* includes all the morphological variations of this taxon; Mediterranean species = *Spiniferites belerius* + *Operculodinium centrocarpum* + *S. bentorii* + *S. mirabilis* + *S. ramosus.* The percentage of freshwater algae is calculated relative to the sum of all dinocysts and freshwater algae, whereas percentages of dinocysts are calculated relative to the total count of dinocyst specimens. The larger variation in dinocyst concentrations at the top of the core is partly due to lower counts of cysts in some samples. Key Mediterranean ostracoda = *Leptocythere ramosa* + *Leptocythere* sp. + *Callistocythere diffusa* + *Palmoconcha* aff. *guttata* + *Cytheroma marinovi.* Key Caspi-brackish ostracoda = *Loxoconcha* aff. *lepida* + *Candona* aff. *schweyeri* + *Callistocythere quinquetuberculata* + *Loxoconcha* sp. + *Eucytherura* sp. These are reported as percentages of all specimens of ostracoda in each sample.

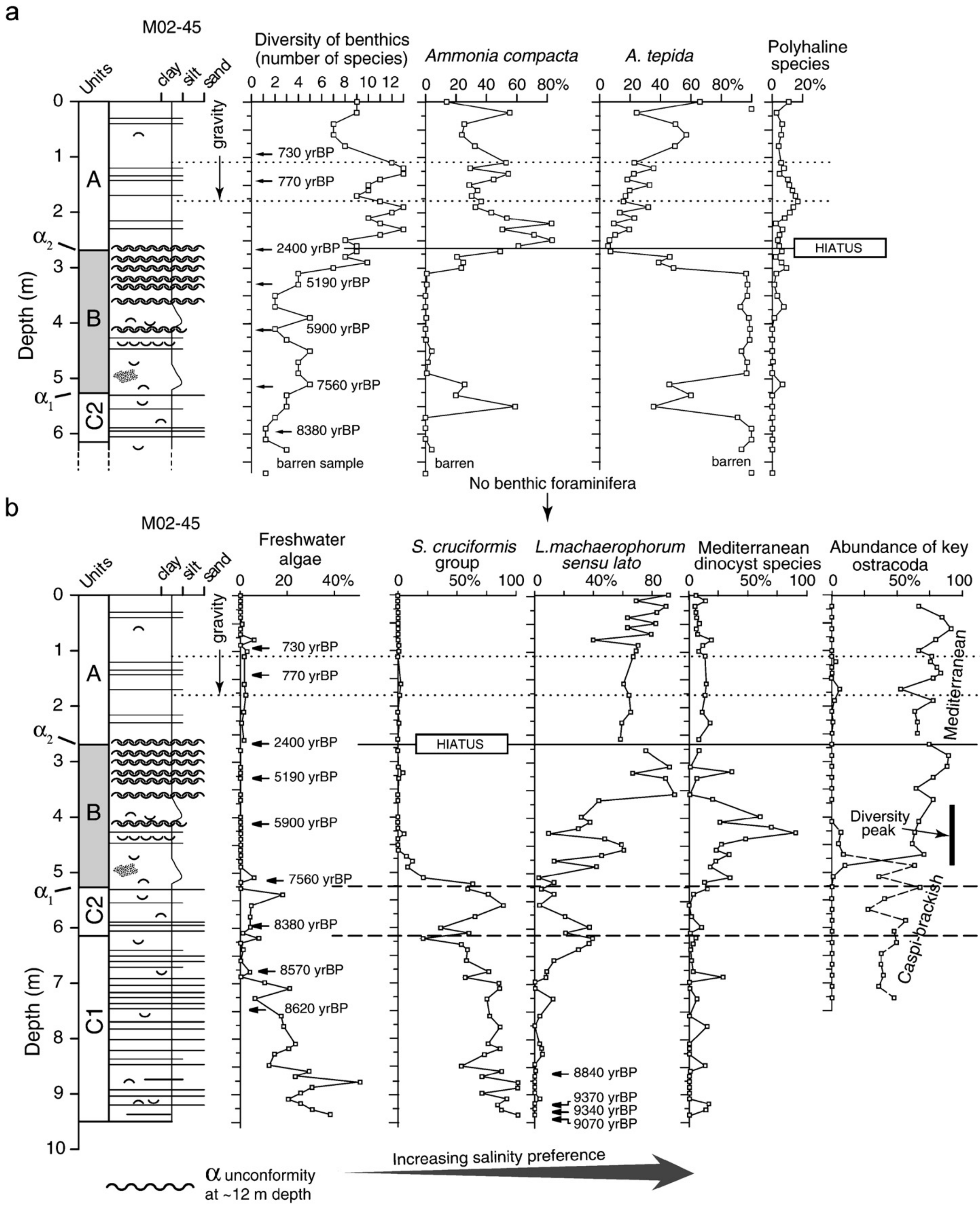
a
M02-45
Units
clay silt sand
gravity
Depth (m)
Diversity of benthics (number of species)
Ammonia compacta
A. tepida
Polyhaline species
730 yrBP
770 yrBP
2400 yrBP
5190 yrBP
5900 yrBP
7560 yrBP
8380 yrBP
barren sample
barren
HIATUS
No benthic foraminifera
b
Freshwater algae
S. cruciformis group
L.machaerophorum sensu lato
Mediterranean dinocyst species
Abundance of key ostracoda
8570 yrBP
8620 yrBP
8840 yrBP
9370 yrBP
9340 yrBP
9070 yrBP
Diversity peak
Mediterranean
Caspi-brackish
Increasing salinity preference
α unconformity at ~12 m depth

in the lower part of Unit B. These species require salinities above 12‰; abundance peaks of these flora indicate sea-surface salinities of at least 20‰. The overlapping occurrences of these Mediterranean species with the *S. cruciformis* assemblage and ostracods with Caspian (brackish) affinities might indicate lower salinities in nearshore areas including the middle shelf, and more influence of Mediterranean waters farther offshore.

Lingulodinium machaerophorum (Fig. 9) can tolerate salinities as low as 3‰, but becomes abundant at salinities >10‰. This acme is confined to core depths shallower than 475 cm (~7000 yr BP), essentially coincident with the proliferation in Unit B of Mediterranean species of molluscs, ostracods and dinocysts. An essentially coincident transition from brackish to more salinity-tolerant dinocysts has been reported for cores collected in coastal areas and the Black Sea shelf off Bulgaria (Filipova-Marinova and Bozilova, 2002; Filipova-Marinova, 2003a; Filipova-Marinova et al., 2004). Unfortunately, use of acetolysis for palynological processing reduces the diversity of dinocysts in these Bulgarian cores (Mudie et al., this volume) and prevents assessment of possible flickering intervals of Mediterranean-type dinocysts during the early Holocene.

6. Discussion of the depositional history

Two issues are critical to an assessment of whether the results from core M02-45 contradict the *Flood Hypothesis* of Ryan et al. (2003) and Major et al. (2006). First, it is essential that the pre-8.4 ka strata accumulated beneath waters of the open Black Sea, rather than in an isolated lake perched at some higher level. Second, the minimum water depth at the core site should have been tens of meters; otherwise, the ~9.3 ka deposits might only require that sealevel was incrementally higher than the −95 m postulated by Ryan et al. (2003), relegating our disagreement with those authors to a matter of 'details' rather than 'substance'.

The time-structure map on the α unconformity confirms an unimpeded connection between the M02-45 coresite and the open Black Sea basin at 9.3 ka. As confirmation, the arrival of the dinocyst *L. machaerophorum* at this location before 8.4 ka (Fig. 9) seemingly requires a free connection between the coresite and the rest of the Black Sea. On the second issue of water depth, we rely on two observations: (1) the Unit C deposits indicate accumulation below storm wave base, and (2) on the modern shelf, accumulation in water depths less than ~50–60 m is prevented by wave agitation (Hiscott and Aksu, 2002). Even if we take account of the somewhat greater protection of the 9.3 ka middle shelf, compared with today, by an offshore bathymetric high (Fig. 3), it does not seem unreasonable to suggest that water depths at the M02-45 coresite were already in excess of ~30–40 m by 9.3 ka. If true, then the Black Sea level would have been shallower than ~−40 to −50 m. Such a level is entirely at odds with the suggestions of Ryan et al. (2003), but is very close to the spill depth required to connect the Black Sea to the Mediterranean. Downstream observations in the Marmara Sea, in particular the timing of sapropel deposition and persistent dysoxia (Çağatay et al., 2000; Kaminski et al., 2002), are compelling evidence that there was unrestricted Black Sea outflow through the Bosphorus Strait from 10.6 to 6.4 ka, including the entire period of Unit C depositon. For such outflow to have occurred, the Black Sea level must have been at least −30 to −40 m in order to overtop the sill in the Bosphorus Strait.

Arguments above convince us that the Holocene transgression of the SW Black Sea shelf began before 10 ka, leading to overspill into the Marmara Sea by ~10.6 ka. After this sealevel rise, the Black Sea remained high until the present. This latter conclusion is supported by Balabanov (2006), Filipova-Marinova (2006) and Yanko-Hombach (2006) who conclude that the Black Sea was never lower than ~−40 m after ~10 ka. In apparent contrast to these ideas, Lericolais et al. (2006) have interpreted buried sediment ridges on the nearby Romanian shelf to be coastal (i.e., subaerial) sand dunes which existed at what is now a depth of about −100 m shortly after the Younger Dryas climatic cooling event (~11–10 ka, uncalibrated). Such subaerial deposits likely exist even in the vicinity of coresite M02-45, along the α unconformity at the base of seismic Unit 1B, but they must be older than 9.5 ka and possibly older than ~10 ka (Fig. 5).

By ~8.4 ka, the outflow weakened sufficiently for the first significant pulse of Mediterranean water to enter the Black Sea. This event is recorded in calcareous shells by a sharp shift to open-ocean strontium isotopic ratios (Major, 2002; Ryan et al., 2003; Major et al., 2006). Likewise, dramatic shifts in fatty acid $\delta^{13}C$ suggest profound changes in water column productivity of the Black Sea at this time. Increased autochthonous production might have accompanied changes in nutrient abundance brought about by this initial pulse of Mediterranean water, but changes in the planktonic and bacterial community structure might also have occurred. If the connection to the Mediterranean had been permanent and complete, then the influx of seawater sulfate would have provided the conditions for sulfate-reducing bacteria to thrive. These bacteria reduce sulfate to sulfide during early diagenesis, with a sulfur isotopic shift of ~−40‰. Remarkably, $\delta^{34}S$ does not plummet in Subunit C2, but actually rises to ~30‰. We believe that this shift to positive values requires the quantitative precipitation of all the new sulfate as sulfide, so that the final $\delta^{34}S$ ratio in the sediments would be identical to the ratio in the incoming seawater. If, instead, there had been a continuous renewal of open-ocean sulfate, then the $\delta^{34}S$ values in the sediments would be shifted by ~−40‰ relative to seawater, leading to highly negative values in the sediments. This did not occur, providing support for the notion that the first Mediterranean influx was brief and short-lived. It was enough to shift the $^{87}Sr/^{86}Sr$ ratio of the Black Sea watermass to open-marine values, but not enough to maintain an isotopic offset between a 'heavy' reservoir of seawater sulfate and a 'light' reservoir in the sulfide minerals in the sediments. The different behavior of strontium and sulfur results from the fact that strontium is a 'trace element' in calcareous shells, whereas sulfur is a relatively more abundant 'minor element' in seawater and in sediments. Strontium ratios would have shifted to open-ocean values with a small influx of Mediterranean water because the strontium concentration in marine water is about two orders of magnitude higher than in fresh water. The strontium isotopic ratios would have remained at open-ocean values for a long period of time because little is removed during biogenic precipitation of carbonate shells. In contrast, newly introduced sulfate would have been rapidly consumed by sulfate-reducing bacteria and potentially entirely removed from the water column.

The proposal that an initial short-lived pulse of seawater enter the Black Sea is supported by trends in the percentages of salinity-diagnostic groups of dinocysts and freshwater algae (Fig. 9). Between ~8.5 and ~8.1 ka, *L. machaerophorum* increased at the expense of the *S. cruciformis* group and freshwater algae (ages are based on the convertion of core depths to time using Fig. 5). This floral shift was temporarily reversed starting at ~8.1 ka (Fig. 9b), but later (~7.5–7.0 ka) the taxa characteristic of lower salinities were completely displaced. Caspi-brackish ostracoda gave way to Mediterranean species and the foraminiferal fauna becames established during this second and larger seawater incursion. Balabanov (2006) also describes this initial pulse, then decline, in the early influx of Mediterranean water from cores collected on the Caucasus shelf (northern Black Sea). There, the first euryhaline immigrants died off at ~8.3–8.2 ka (compare Fig. 9b), then returned in larger numbers a short time later. Filipova-Marinova (2003a, 2006) likewise notes the occurrence of single specimens of euryhaline gastropods and small numbers of euryhaline dinoflagellate cysts in pre-8.4 ka deposits at the mouth of the Veleka River, southern Bulgaria, and attributes these to "an accidental ingress of Mediterranean sea water" at that time.

We believe that the first pulse of Mediterranean water entered the Black Sea at ~8.4 ka not because of a "flood", but because the persistent Black Sea outflow weakened temporarily (see also Balabanov, 2006). The sulfate in this incoming water was entirely reduced and incorporated into the sediments of Subunit C2 where it is now observed as abundant <5 μm particles of pyrite (Mudie et al., this volume). The peak in TS at this time is followed by a decline toward the top of the subunit. δ^{34}S in the sediments rose to open-ocean values because bacterial fractionation was negated by extreme substrate limitation and complete conversion of all of the new sulfate to sedimentary sulfide in an essentially closed system (e.g., Londry and Des Marais, 2003). This period is also marked by a significant shift in fatty acid δ^{13}C, reflecting changes in nutrient balance, carbon substrate or microbial community structure in the Black Sea watermass. Some salinity-tolerant dinocysts (e.g., *L. machaerophorum*) might have arrived with this first pulse of saline water. The floral data potentially indicate the arrival of the first immigrants a short time before 8.4 ka (Fig. 9), perhaps during seasonal declines in Black Sea outflow too small to influence the bulk geochemistry of the basinal waters. Corroboration is provided by Balabanov (2006), who notes the presence of "rare larvae and immature species of *Cardium edule*, *Abra ovata*, and, infrequently, *Chione gallina* and *Spisula subtruncata*" in sediments older than ~8.5 ka beneath the northern Black Sea shelf.

At the base of Unit B, several biological and geochemical proxies track the second influx of Mediterranean waters which has persisted to the present day. This influx started at ~7.5 ka and is attributed to the initiation of permanent two-way flow in the Bosphorus Strait. Mediterranean benthic foraminifera, ostracods and molluscs took over from brackish species during a transitional period of ~500 years. The benthic foraminiferal assemblage of Unit B compares best with the modern middle shelf fauna (35–70 m water depth, Bulgarian Shelf) reported by Yanko (1990, Tables 1 and 2), whereas the foraminiferal assemblage of Unit A compares best with her deeper shelf assemblage found at water depths in excess of 70 m. Sulfate concentrations rose sufficiently just before the onset of Unit B deposition to nourish an active crop of sulfate-reducing bacteria in surface sediments, leading to a pronounced drop in δ^{34}S values to an average of ~−20‰ (Fig. 7b).

There is no debate concerning the post-7.5 ka arrival and proliferation of Mediterranean species on shelves of the Black Sea. Ryan et al. (1997) originally flagged this proliferation as evidence for a catastrophic flood at that time, but later moved the time of flooding back almost 1000 years to 8.4 ka based on strontium isotopes in calcareous shells (Ryan et al., 2003; Major et al., 2006). Instead, we have consistently argued (e.g., Aksu et al., 1999a) that the ~7.5 ka faunal turnover resulted from a time lag between initial reconnection of the Black Sea with the Mediterranean, and the colonization of shelf environments by organisms which experienced difficulty entering the Black Sea because of strong outflow and inhospitable environmental conditions (e.g., low salinity).

Ryan et al. (2003) criticized our contention that strong outflow could have prevented immigration of Mediterranean aquatic organisms into the Black Sea. They stated that "Although one could argue that Black Sea discharge to the Marmara Sea was so strong as to keep the saltwater out, the Marmara Sea passes this same stream to the Mediterranean via the Dardanelles Strait. Yet the Marmara Sea did not keep the Mediterranean at bay but became marine at 11.7 ky BP as soon as its outlet was breached". This criticism has no merit whatsoever, because no one has proposed that the Black Sea was exporting fresh water to the Mediterranean at 11.7 ka (Fig. 1). Instead, the Marmara Sea was an isolated lake which became a marine embayment of the Aegean Sea after it was passively flooded at ~12 ka (Çağatay et al., 2000; Hiscott and Aksu, 2002).

During its reconnection to the Mediterranean, there was no outflow through the Dardanelles; the Marmara Sea might actually have been abruptly inundated because its level was lower than that of the open ocean by ~15 m (Hiscott and Aksu, 2002).

In core M02-45, the record of conditions from ~4.5 to 2.5 ka is apparently missing at unconformity α_2. Above α_2 in Unit A, TS is very low compared to underlying values, consistent with deposition in a poorly oxygenated basin where sulfur is removed and deposited as pyrite in deep-water areas. On the shelf, pore-water sulfate is also reduced to sulfide during early diagenesis, with the bacterial fractionation accounting for persistently low δ^{34}S values of ~−20‰ (Fig. 7b).

7. Origin of α_1 and α_2

In our earlier work (Aksu et al., 2002a) and in other studies (Ryan et al., 2003), it has been proposed that unconformities above α were created by erosion during times of lower water level, perhaps even during times of subaerial exposure and subsequent transgressive erosion (ravinement). Indeed, there is evidence elsewhere in the Black Sea for minor transgressions and regressions throughout the Holocene (Chepalyga, 1984; Filipova-Marinova, 2003a, 2006; Balabanov, 2006; Ivanov and Kakaranza, 2006). However, we now believe that water level changes are not essential to the development of α_1 and α_2. Instead, we hypothesize that unconformities like α_2 develop on the inner and middle shelf wherever surface currents are strong enough to prevent deposition.

Today, the SW Black Sea shelf is swept by the Rim Current and an associated set of semi-permanent eddies (Oğuz et al., 1993). Can this current cause local erosion? As part of a separate study of the seabed seaward of the Bosphorus exit into the Black Sea, we have acquired a multibeam mosaic, including backscatter imagery (Hiscott et al., 2006). Approximately 35 km^2 of the seabed in the multi-beam survey area is characterized by surface lineations which result from truncation of shallowly dipping strata equivalent to Unit A. This beveled seabed is a "modern" unconformity that is being created under modern oceanographic conditions, and which will surely be buried in the future to produce a stratal discontinuity very similar to α_1 or α_2. The second point in our argument against a sealevel control on α_1 and α_2 is the geographic restriction of these hiatuses to local areas. If they were the result of water-level changes, then we would expect them to be widespread across the shelf. Seaward of the Sakarya River delta, Algan et al. (2002) record no unconformity younger than 7–8 ka. As corroboration, we have unpublished radiocarbon ages obtained on mollusc shells in long piston cores in the same area (Aksu et al., 2006) that demonstrate uninterrupted sedimentation precisely when α_2 was developing at coresite M02-45 (i.e., in the interval 4.5–2.5 ka). These observations are, in our view, inconsistent with a basin-wide regression as the cause for this unconformity.

As a final point, Giosan et al. (2006) have determined from study of the Danube Delta that the water level of the Black Sea has not varied by more than a few meters in the last 5000 years. They argue that younger water-level excursions reported by other workers are likely attributable to local subsidence rather than basin-scale sealevel changes. Our reinterpretation of the origin of unconformities α_1 and α_2 is consistent with their view.

It might be possible that the Holocene Rim Current system reorganized itself from time to time as water-mass characteristics or wind patterns in the region changed. We are not aware of physical oceanographic data which would bear on the issue of long-term stability of the surface currents in the Black Sea, so our hypothesis of periodic reorganization is necessarily somewhat speculative.

8. Conclusions

The major conclusion that we draw from the study of core M02-45 is that the SW Black Sea shelf was transgressed by no later than 10 ka, and that the outer and middle shelf has been under water ever since. This conclusion accords with the published results of many Russian, Bulgarian and Ukrainian workers (Chepalyga, 1984; Balabanov, 2006; Murdmaa et al., 2006; Yanko-Hombach, 2006) but is in direct conflict with the Flood Hypothesis of Ryan et al. (2003) and Major et al. (2006). The deepest facies in the core (age = ~9.3 ka) was apparently deposited below storm wave base as prodelta muds and turbidites, implying that the level of the Black Sea was near or at the sill depth of the Bosphorus Strait throughout the Holocene. The reconnection to the Mediterranean Sea involved a number of steps and mostly progressive changes from one stage to the next. From ~10 to 8.4 ka, we infer that the Black Sea was flowing so strongly out through the Bosphorus Strait that no Mediterranean water penetrated northward—early in this period, the Marmara Sea would have been lower than the Black Sea so that the Bosphorus would have been a river with a significant surface slope toward the south. At ~8.4 ka, a first pulse of Mediterranean water entered the Black Sea, perhaps because of a temporary decline in riverine inflow from northern European watersheds. This pulse was sufficient to permanently (until today) shift the strontium isotopic signature of the Black Sea to global values, but the newly introduced sulfate was rapidly consumed by sulfate-reducing bacteria and buried as pyrite in Subunit C2 (and contemporaneous) sediments. Because all the sulfate was consumed, the sedimentary sulfur is unfractionated relative to seawater. Finally, at ~7.5 ka, outflow declined enough to permit continuous two-way flow throught the strait, opening the Black Sea to a wide variety of Mediterranean immigrant species, and leading to the establishment of a typical marine diagenetic profile with active sulfate reduction, strong sulfur isotopic fractionation, and negative $\delta^{34}S$ values in the sediments. By the time that onlapping sediments buried the α_2 unconformity at ~2.5 ka, the middle shelf was a dyaerobic setting, perhaps because of a progressive rise of the chemocline. The timing of this transition is poorly constrained at coresite M02-45 because of the hiatus at unconformity α_2, which we attribute to intensification of the Rim Current during the middle Holocene.

Proxy data from core M02-45 are therefore entirely consistent with the Outflow Hypothesis of Hiscott et al. (2007). Our conclusion that the Holocene was moist and that water levels remained high is corroborated by the pollen records for core M02-45, core B7 (from the southern Black Sea basin), and coastal areas of southeastern Bulgaria that clearly show the onset of (i) humid conditions supporting mesic forest, and (ii) relatively warm winter conditions (>5 °C) by 9 ka (Mudie et al., 2002b; Filipova-Marinova, 2003b; Mudie et al., this volume). These pollen data are inconsistent with the cold dry conditions postulated by Ryan et al. (2003) to account for the early Holocene drawdown. The only change we would make to Fig. 1b is to shift the onset of fully developed two-way flow from ~8.4 to ~7.5 ka.

Acknowledgments

We thank the officers and crew of the R.V. Koca Piri Reis for invaluable assistance during a succession of successful cruises. Hiscott and Aksu acknowledge funding and in-kind support from the Natural Sciences and Engineering Research Council of Canada, the Piri Reis Foundation, the Geological Survey of Canada, and the Vice-President (Research) of Memorial University of Newfoundland. Kaminski thanks the Graduate School of the University College of London for grant funds. Evans was able to participate in this project through support from a Natural Environment Research Council (UK) studentship. An anonymous reviewer and special-issue editor Valentina Yanko-Hombach are thanked for their constructive criticisms that improved the paper.

References

Abbott, R.T., Dance, S.P., 1998. Compendium of Seashells. Odyssey Publishing, Hong Kong, 412p.

Abrajano, T., Aksu, A.E., Hiscott, R.N., Mudie, P.J., 2002. Aspects of carbon isotope biogeochemistry of Late Quaternary sediments from the Marmara Sea and Black Sea. Marine Geology 190, 151–164.

Aksu, A.E., Hiscott, R.N., Yaşar, D., 1999a. Oscillating Quaternary water levels of the Marmara Sea and vigorous outflow into the Aegean Sea from the Marmara Sea–Black Sea drainage corridor. Marine Geology 153, 275–302.

Aksu, A.E., Abrajano, T., Mudie, P.J., Yaşar, D., 1999b. Organic geochemical and palynological evidence for terrigenous origin of the organic matter in Aegean Sea sapropel S1. Marine Geology 153, 303–318.

Aksu, A.E., Hiscott, R.N., Yaşar, D., Işler, F.I., Marsh, S., 2002a. Seismic stratigraphy of Late Quaternary deposits from the southwestern Black Sea shelf: evidence for non-catastrophic variations in sea-level during the last 10,000 years. Marine Geology 190, 61–94.

Aksu, A.E., Hiscott, R.N., Mudie, P.J., Rochon, A., Kaminski, M.A., Abrajano, T., Yaşar, D., 2002b. Persistent Holocene outflow from the Black Sea to the Eastern Mediterranean contradicts Noah's Flood hypothesis. GSA Today 12 (5), 4–10.

Aksu, A.E., Hiscott, R.N., Mudie, P.J., Kaminski, M.A., Abrajano, T., Marret, F., Yaşar, D., 2006. Pre-10 ka transgression of the SW Black Sea shelves: seismic and core evidence. In: IGCP 521 Second Plenary Meeting, Odessa, Ukraine, 20–28 August, Abstracts volume, pp. 4–6.

Algan, O., Gökaşn, E., Gazioğlu, C., Yücel, Z.Y., Alpar, B., Güneysu, C., Kirci, E., Demirel, S., Sari, E., Ongan, D., 2002. A high-resolution seismic study in Sakarya Delta and Submarine Canyon, southern Black Sea shelf. Continental Shelf Research 22, 1511–1527.

Athersuch, J., Horne, D.J., Whittaker, J.E., 1989. Marine and Brackish Water Ostracods. E.J. Brill, Bath, UK, 343p. + 7 plates.

Balabanov, I.P., 2006. Holocene sea-level changes in the northern Black Sea. In: IGCP 521 Second Plenary Meeting, Odessa, Ukraine, 20–28 August, Abstracts volume, pp. 21–23.

Çağatay, M.N., Görür, N., Algan, O., Eastoe, C., Tchepalyga, A., Ongan, D., Kuhn, T., Kuşcu, I., 2000. Late Glacial–Holocene palaeoceanography of the Sea of Marmara: timing of connections with the Mediterranean and Black Seas. Marine Geology 167, 191–206.

Çakiroğlu, A.İ., 2005. Distribution of mollusc assemblages in the surface sediments of the Black Sea, Marmara Sea and Aegean Sea. M.Sc. Thesis, Memorial University of Newfoundland, St. John's, Canada, 220p.

Chepalyga, A.L., 1984. Inland Sea basins. In: Barnosky-Cathy, W. (Ed.), Late Quaternary Environments of the Soviet Union. University of Minnesota Press, Minneapolis, MN, pp. 229–247 (Chapter 23).

Demir, M., 2003. Shells of Mollusca collected from the Seas of Turkey. Turkish Journal of Zoology, TÜB〈TAK 27, 101–140.

Evans, J.M., 2004. Noah's Flood: fact or fiction? A palaeoenvironmental study of Holocene Black Sea ostracoda. M.Sc. in Micropalaeontology project report, University College London, 79p.

Filipova-Marinova, M., 2003a. Paleoenvironmental changes along the Southern Black Sea Coast of Bulgaria during the last 29000 years. Phytologia Balcanica 9, 275–292.

Filipova-Marinova, M., 2003b. Postglacial vegetation dynamics in the coastal part of the Strandza Mountains, southeastern Bulgaria. In: Tonkov, S. (Ed.), Aspects of Palynology and Palaeoecology: Festschrift in honour of Elissaveta Bozilova. PENSOFT Publishers, Sofia, Bulgaria, pp. 213–231.

Filipova-Marinova, M., 2006. Archaeological and paleontological evidence of climate dynamics, sealevel change, and coastline migration in the Bulgarian sector of the circum-Pontic region. In: Yanko-Hombach, V., Gilbert, A.S., Panin, N., Dolukhanov, P. (Eds.), The Black Sea Flood Question: Changes in Coastline, Climate, and Human Settlement. Springer, Dordrecht, The Netherlands, pp. 453–481.

Filipova-Marinova, M., Bozilova, E., 2002. Paleoecological conditions in the area of the prehistorical settlement in the Bay of Sozopol during the Eneolithic. Phytologia Balcanica 8 (2), 133–143.

Filipova-Marinova, M., Christova, R., Bozilova, E., 2004. Palaeoeological conditions in the Bulgarian Black Sea area during the Quaternary. Journal Environmental Micropaleontology, Microbiology and Meiobenthology 1, 135–154.

Fairbanks, R.G., 1989. A 17,000-year glacio-eustatic sea level record: influence of glacial melting rates on the Younger Dryas event and deep-ocean circulation. Nature 342, 637–642.

Fedorov, P., 1982. Nekotorye diskusionnye voprosy pleistotsenovoi istorii Chernogo moria [Some controversial questions about the Pleistocene history of the Black Sea]. Buletin Moskovskogo obshchestva ispytatelei prirody, otdelenie geologicheskoe 57 (1), 108–117 (In Russian).

Giosan, L., Donnelly, J.P., Constantinescu, S., Filip, F., Ovejanu, I., Vespremeanu-Stroe, A., Vespremeanu, E., Duller, G.A.T., 2006. Young Danube delta documents stable Black Sea level since the middle Holocene: morphodynamic, paleogeographic, and archaeological implications. Geology 34, 757–760.

Graham, A., 1971. British Prosobranch and Other Operculate Gastropod Molluscs. The Linnean Society of London, Academic Press, London and New York, 112p.

Grossu, A.V., 1995. Fauna Republiciipopulare Romîne: Mollusca. V.III. Academiei Republicii Populare Romîne.

Hiscott, R.N., Aksu, A.E., 2002. Late Quaternary history of the Marmara Sea and Black Sea from high-resolution seismic and gravity-core studies. Marine Geology 190, 261–282.

Hiscott, R.N., Aksu, A.E., Yaşar, D., Kaminski, M.A., Mudie, P.J., Kostylev, V., MacDonald, J., Işler, F.I., Lord, A.R., 2002. Deltas south of the Strait of Bosphorus record persistent Black Sea outflow to the Marmara Sea since ~10 ka. Marine Geology 190, 95–118.

Hiscott, R.N., Aksu, A.E., Mudie, P.J., Kaminski, M.A., Abrajano, T., Yaşar, D., Rochon, A., 2007. The Marmara Sea Gateway since ~16 ka: non-catastrophic causes of paleoceanographic events in the Black Sea at 8.4 ka and 7.15 ka. In: Yanko-Hombach, V., Gilbert, A.S., Panin, N., Dolukhanov, P. (Eds.), The Black Sea Flood Question: Changes in Coastline, Climate, and Human Settlement. Springer, Dordrecht, The Netherlands, pp. 89–117.

Hiscott, R.N., Flood, R.D., Aksu, A.E., Kinney, J., Yaşar, D., 2006. Saline density-current channel created by Mediterranean inflow to the Black Sea through the Bosphorus Strait: morphology, history, and surface-current modification imaged by swath mapping and Huntec boomer profiles. Abstract, International Congress of Sedimentology, Fukuoka, Japan.

Ivanov, V.G., Kakaranza, S.D., 2006. Major stages of Late Pleistocene–-Holocene evolution of the northwestern Black Sea. In: IGCP 521 Second Plenary Meeting, Odessa, Ukraine, 20–28 August, Abstracts volume, pp. 75–80.

Kaminski, M.A., Aksu, A.E., Hiscott, R.N., Box, M., Al-Salameen, M., Filipescu, S., 2002. Late glacial to Holocene benthic foraminifera in the Marmara Sea: implications for Black Sea – Mediterranean Sea connections following the last deglaciation. Marine Geology 190, 165–202.

Khrischev, K.V., Georgiev, V., 1991. Regional washout in the Pleistocene–Holocene boundary in the western Black Sea depression. Comptes rendus de l'Académie bulgare des Sciences 44 (9), 69–71.

Lericolais, G., Bulois, C., Gillet, H., 2006. Coastal sand dunes at −100 m under sea level as proof of a post Younger-Dryas Black Sea lowstand. In: IGCP 521 Second Plenary Meeting, Odessa, Ukraine, August 20–28, Abstracts volume, pp. 108–110.

Londry, K.L., Des Marais, D.J., 2003. Stable carbon isotope fractionation by sulfate reducing bacteria. Applied and Environmental Microbiology 69, 2942–2949.

Major, C.O., 2002. Non-eustatic controls on sealevel change in semi-enclosed basins. Ph.D. Thesis. Columbia University, NY. 223p.

Major, C.O., Goldstein, S.L., Ryan, W.B.F., Lericolais, G., Piotrowski, A.M., Hajdas, I., 2006. The co-evolution of Black Sea level and composition through the last deglaciation and its paleoclimatic significance. Quaternary Science Reviews 25, 2031–2047.

Mart, Y., Ryan, W., Çağatay, N., McHugh, C., Giosan, L., Vachtman, D., 2006. Evidence for intensive flow from the Bosporus northwards during the early Holocene. Geophysical Research Abstracts, 8, SRef-ID: 1607-7962/gra/EGU06-A-02572.

Mudie, P.J., Rochon, A., Aksu, A.E., Gillespie, H., 2002a. Dinoflagellate cysts and freshwater algae and fungal spores as salinity indicators in Late Quaternary cores from Marmara and Black Seas. Marine Geology 190, 203–231.

Mudie, P.J., Rochon, A., Aksu, A.E., 2002b. Pollen stratigraphy of Late Quaternary cores from Marmara Sea: land–sea correlation and paleoclimatic history. Marine Geology 190, 233–260.

Mudie, P.J., Rochon, A., Aksu, A.E., Gillespie, H., 2004. Late glacial, Holocene and modern dinoflagellate cyst assemblages in the Aegean–-Marmara–Black Sea corridor: statistical analysis and re-interpretation of the early Holocene Noah's Flood hypothesis. Review of Palaeobotany and Palynology 128, 143–167.

Müller, G.I., 1995. Diversitatea Lumii VII—Determinatorul ilustrat al florei fli faunei României sub redactia Stoica Preda Godeanu, Volumul I—Mediul Marin, pp. 197–221.

Murdmaa, I., Ivanova, E., Chepalyga, A., Cronin, T., Levchenko, O., Howe, S., Manushkina, A., Pasechnik, I., Platonova, E., 2006. Paleoenvironments on the north Caucasian Black Sea shelf since the LGM. In: IGCP 521 Second Plenary Meeting, Odessa, Ukraine, 20–28 August, Abstracts volume, pp. 127–129.

Oğuz, T., Latun, V.S., Latif, M.A., Vladimirov, V.V., Sur, H.I., Markov, A.A., Özsoy, E., Kotovshchikov, B.B., Eremeev, V.V., Ünlüata, Ü., 1993. Circulation in the surface and intermediate layers of the Black Sea. Deep-Sea Research I 40, 1597–1612.

Paytan, A., Kastner, M., Campbell, D., Thiemens, M.H., 1998. Sulfur isotopic composition of Cenozoic seawater sulfate. Science 282, 1459–1462.

Poppe, G.T., Goto, Y., 1991. European Seashells. Volumes I and II, Verlag Christa Hemmen, Wiesbaden, Germany, 352pp, 221pp.

Ryan, W.B.F., Pitman III, W.C., Major, C.O., Shimkus, K., Maskalenko, V., Jones, G.A., Dimitrov, P., Görür, N., Sakinç, M., Yüce, H., 1997. An abrupt drowning of the Black Sea shelf. Marine Geology 138, 119–126.

Ryan, W.B.F., Major, C.O., Lericolais, G., Goldstein, S.L., 2003. Catastrophic flooding of the Black Sea. Annual Review Earth and Planetary Sciences 31, 525–554.

Schornikov, E.N., 1967. Identification Key to the Fauna of the Black Sea and Azov Sea. Volume 2: Free Living Invertebates. Crustacean. 12 Datel'Stvo, Kiev, Russia, 536pp.

Tebble, N., 1966. British Bivalve Seashells. A handbook for identification. Trustees of British Museum (Natural History), 212pp.

Yanko-Hombach, V., 2006. Transformation of the Neoeuxinian lake into the Black Sea: evidence from benthic foraminifera. In: IGCP 521 Second Plenary Meeting, Odessa, Ukraine, 20–28 August, Abstracts volume, pp. 171–173.

Yanko, V., 1990. Stratigraphy and paleogeography of the marine Pleistocene and Holocene deposits of the southern seas of the USSR. Memorie Società Geologica Italiana 44, 167–187.

Yanko, V.V., Troitskaya, T.S., 1987. Late Quaternary foraminifera of the Black Sea. Akademia Nauk SSSR, Sibirskoye Otdeleniye, Institut Geologii i Geofizikii im. 60-letiya Soyuza SSR, Trudy, vypusk 694. Nauka Publishers, Moscow, 111p. [in Russian].